

Monte Carlo Studies of Three-Dimensional Bond-Diluted Ferromagnets

P.-E. Berche¹, C. Chatelain^{2,3}, B. Berche² and W. Janke³

¹ Groupe de Physique des Matériaux, Université de Rouen, F-76821 Mont Saint-Aignan Cedex, France
pierre.berche@univ-rouen.fr

² Laboratoire de Physique des Matériaux, Université Henri Poincaré, Nancy I, BP 239, F-54506 Vandœuvre les Nancy Cedex, France
chatelai, berche@lpm.u-nancy.fr

³ Institut für Theoretische Physik, Universität Leipzig, Augustusplatz 10/11, D-04109 Leipzig, Germany
christophe.chatelain, wolfgang.janke@itp.uni-leipzig.de

1 Introduction

The influence of quenched, random disorder on phase transitions is of great importance in a large variety of fields [1], ranging from experiments with absorbed monolayers [2] in condensed matter physics to conceptual questions in non-perturbative quantum gravity [3].

For pure systems exhibiting a *continuous* phase transition, Harris [4] derived the criterion that random disorder is a relevant perturbation when the critical exponent of the specific heat of the pure system is positive, $\alpha_{\text{pure}} > 0$. In this case one expects that the system falls into a new universality class with critical exponents governed by a “disordered” fixed point. For $\alpha_{\text{pure}} < 0$ the behaviour of the pure system should persist, and $\alpha_{\text{pure}} = 0$ is a special, marginal case. In two dimensions (2D) this scenario has been confirmed by various methods for many different systems [5]. In three dimensions (3D) extensive computer simulation studies have concentrated mainly on the *site-diluted* Ising model [5, 6].

If a pure system with a *first-order* phase transition is subject to quenched disorder, the transition is softened and may even turn into a continuous one [7]. This is always the case in 2D [8]; for numerical verifications see Refs. [9-13]. In higher dimensions, a tricritical point may appear at a finite concentration of impurities [14], separating “non-softened” first-order and “softened” second-order regimes [15]. Numerically such a scenario has recently been observed for the 3D *site-diluted* 3-state Potts model [16]. Since the first-order transition of the pure version of this model is very weak [17], however, the characterization of the tricritical point remained inconclusive.

In this report we give an overview on recent results obtained from extensive Monte Carlo (MC) computer simulations of the 3D 2-state (Ising) [18] and 4-state Potts [19-21] models with *bond-dilution*. The motivation to

study the 4-state Potts model derives from the fact that, in the pure case, this model is known to exhibit a fairly strong first-order transition, such that a disorder-induced softening to a second-order transition would give clear support for the theoretical picture sketched above. Modeling the disorder by bond-dilution enables in the Ising case a test of the expected universality with respect to the type of disorder. Furthermore, for both models this choice facilitates a quantitative comparison with recent high-temperature series expansions [22, 23] for general random-bond q -state Potts models.

2 Model and Simulation Setup

The 3D bond-diluted q -state Potts model is defined by the Hamiltonian

$$-\beta H = \sum_{\langle ij \rangle} K_{ij} \delta_{\sigma_i, \sigma_j}; \quad \sigma_i = 1, \dots, q, \quad (1)$$

where the sum extends over all pairs of neighbouring sites on a cubic lattice of size L^3 with periodic boundary conditions, and the couplings K_{ij} are distributed according to the distribution

$$\wp(K_{ij}) = p \delta(K_{ij} - K) + (1 - p) \delta(K_{ij}), \quad (2)$$

where $K \equiv J/k_B T$ is the inverse temperature in natural units. The dilution parameter p is thus the concentration of magnetic bonds in the system, i.e., $p = 1$ corresponds to the pure case. Below the percolation threshold $p_c = 0.248\,812\,6(5)$ [24] one does not expect any finite-temperature phase transition since without any percolating cluster in the system long-range order is impossible.

The model (1), (2) was studied by means of large-scale MC simulations using the Swendsen-Wang (SW) cluster algorithm [25] in the regime of second-order transitions, and multicanonical simulations [26, 27] in the regime where the first-order transition of the pure 4-state Potts model persists, i.e., at weak dilution close to $p = 1$. Thermodynamic quantities were averaged over a large number of quenched disorder realisations, ranging between 2 000 and 5 000. The stability of the disorder averages has been checked by monitoring running averages as a function of the number of random samples. In fact, some care is necessary because too small a number of disorder realisations would lead to *typical* values rather than average ones [28], and these two values are different if the probability distribution over the disorder realisations exhibits a long tail.

3 Results

3.1 3D Bond-Diluted Ising Model

The phase diagram of the 3D bond-diluted Ising model has been obtained numerically from the locations of the maxima of a diverging quantity such as

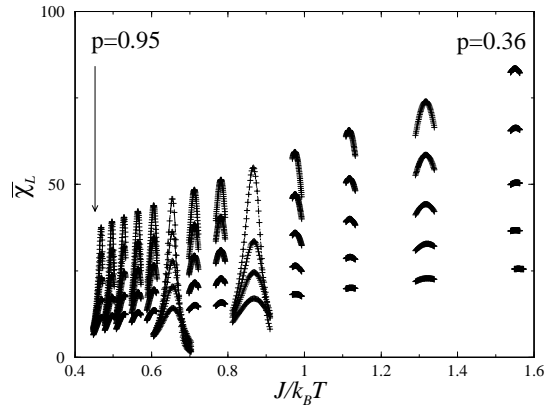


Fig. 1. The average magnetic susceptibility $\bar{\chi}_L$ of the 3D bond-diluted Ising model versus $K = J/k_B T$ for several concentrations p and $L = 8, 10, 12, 14, 16, 18,$ and 20 . For each value of p and each lattice size L , the curves are obtained by standard histogram reweighting of the simulation data at one value of K .

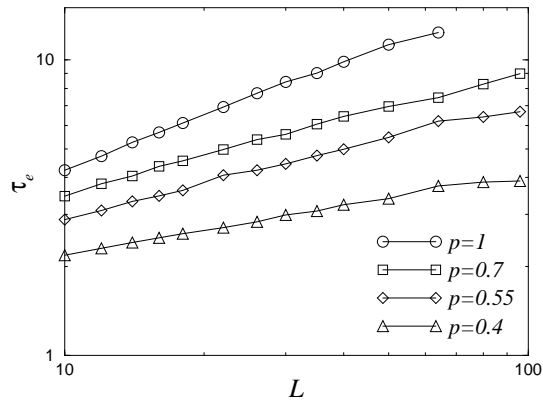


Fig. 2. The energy autocorrelation time τ_e versus the size L of the 3D bond-diluted Ising model with SW cluster-update dynamics for various concentrations of magnetic bonds p on a log-log scale. The pure case corresponds to $p = 1$.

the magnetic susceptibility $\bar{\chi}_L$ depicted in Fig. 1. We focused on $\bar{\chi}_L$ because the stability of the disordered fixed point implies a negative specific-heat exponent in a random system [29]. The error in this quantity is hence typically larger than that in the susceptibility.

For an accurate determination of the maxima of the susceptibility we used the histogram reweighting technique with $N_{\text{MCS}} = 2500$ MC sweeps (MCS) and between $N_s = 2500$ and 5000 disorder realisations. The choice of N_{MCS} is justified by the increasing behaviour of the energy autocorrelation time

Table 1. Evolution of the 3D Ising model susceptibility for $p = 0.7$ and $L = 96$ with the number of MC sweeps, N_{MCS} , for different disorder realisations, χ_j , and the average value over 2 500 realisations, $\bar{\chi}$.

N_{MCS}	χ_1	χ_2	χ_3	χ_4	χ_5	$\bar{\chi}$
100	1 268	720	1 141	939	833	1 058
500	1 272	1 520	1 223	1 029	953	1 210
1 000	1 262	1 544	1 205	1 068	911	1 219
1 500	1 282	1 433	1 277	1 047	915	1 227
2 000	1 332	1 441	1 221	1 073	917	1 235
2 500	1 358	1 484	1 234	1 012	1 014	1 234

τ_e as a function of p and L . At the critical point of a second-order phase transition one expects a finite-size scaling (FSS) behaviour $\tau_e \propto L^z$, where z is the dynamical critical exponent. From fits to the data shown in Fig. 2 we obtained values of $z \approx 0.27, 0.38, 0.41$, and 0.59 for $p = 0.4, 0.55, 0.7$, and 1.0 (the pure case), respectively. The critical slowing down thus weakens for the disordered model and becomes less and less pronounced when the concentration of magnetic bonds p decreases. The largest autocorrelation time observed for the disordered model was around $\tau_e \approx 9$ for $p = 0.7$ and $L = 96$. For each dilution and each size we thus collected at least 250 effectively uncorrelated measurements of the physical quantities, i.e., $N_{\text{MCS}} > 250 \tau_e$. On the other hand, for small $p \approx p_c$ it is necessary to increase the number of disorder realisations because of the vicinity of the percolation threshold.

In order to check the quality of the averaging techniques, we first studied the stability of the susceptibility versus the number of MC sweeps involved in the thermal average. For the largest size considered our results are given

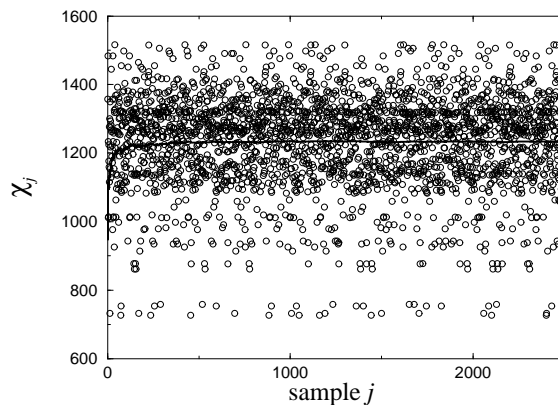


Fig. 3. Distribution of the susceptibility for the different disorder realisations of the 3D Ising model with a concentration of magnetic bonds $p = 0.7$ and $L = 96$. The (running) average value over the samples $\bar{\chi}$ is shown by the solid line.

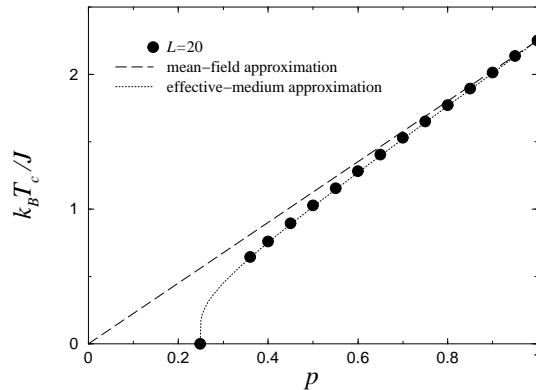


Fig. 4. Phase diagram of the 3D bond-diluted Ising model compared with the mean-field and effective-medium approximations (3) and (4), respectively.

in Table 1 for different samples as well as for the disorder average. With 2500 MCS, the accuracy of the results for a given sample is not perfect, of course, but the precision of the average over disorder is quite good on the other hand. The disorder average procedure has been investigated by computing the susceptibility χ_j for different samples, $1 \leq j \leq N_s$. As can be seen in Fig. 3, the dispersion of the values of χ is not very large because the fluctuations in the (running) average value disappear already after a few hundreds of realisations.

The phase diagram as obtained from the susceptibility maxima for the largest lattice size is shown in Fig. 4. We do not include the results from high-temperature series expansions [22] in this figure since they would just fall on top of the MC data. For comparison we have drawn, however, a simple mean-field (MF) estimate of the transition point,

$$K_c^{\text{MF}}(p) = K_c(1)/p, \quad (3)$$

with $K_c(1) = 0.443\,308\,8(6)$ [30]. This rather crude approximation only holds in the low-dilution regime, $p > 0.8$. On the other hand, the single-bond effective-medium (EM) approximation of Turban [31],

$$K_c^{\text{EM}}(p) = \ln \left[\frac{(1-p_c)e^{K_c(1)} - (1-p)}{p-p_c} \right], \quad (4)$$

gives very good agreement with the simulated transition line over the full dilution range. Since $K_c(1)$ and p_c are input parameters this relation is trivially exact in the vicinity of both the pure system and the percolation threshold.

Due to the competition between different fixed points, one of the main problems encountered in previous studies of the disordered Ising model was

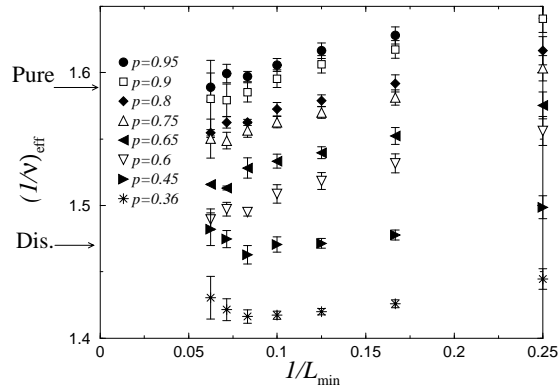


Fig. 5. Effective exponents $(1/\nu)_{\text{eff}}$ as a function of $1/L_{\text{min}}$ for $p = 0.95, 0.9, 0.8, 0.75, 0.65, 0.6, 0.45$, and 0.36 . The error bars show the standard deviations of the power-law fits. The arrows indicate the values of $1/\nu$ for the pure [32] and site-diluted [33] 3D Ising models, respectively.

the question whether one measures effective or asymptotic exponents. Although the change of universality class should happen theoretically for an arbitrarily low disorder, it can be very difficult to measure the new critical exponents because the asymptotic behaviour cannot always be reached practically. Another difficulty comes from the vicinity of the ratios γ/ν and β/ν in the pure and disordered universality classes. Indeed, for the 3D Ising model these values are:

$$\gamma/\nu = 1.966(6), \quad \beta/\nu = 0.517(3), \quad \nu = 0.6304(13) \quad \text{pure case [32]}, \quad (5)$$

$$\gamma/\nu = 1.963(5), \quad \beta/\nu = 0.519(3), \quad \nu = 0.6837(53) \quad \text{disordered case [33]}. \quad (6)$$

Recent field theoretical determinations of critical exponents in the disordered case are presented in Refs. [34, 35], and for an excellent review of various experimental, theoretical and numerical estimates in the last two decades, see Ref. [6]. Thus, from standard FSS techniques, the critical exponent ν only will allow us to discriminate between the two fixed points. This exponent can be evaluated from the FSS behaviour of the derivative of the magnetisation w.r.t. temperature which is expected to behave as $d \ln \bar{m} / dK \propto L^{1/\nu}$. From this power-law behaviour, we have extracted the effective size-dependent exponent $(1/\nu)_{\text{eff}}$ which is plotted in Fig. 5 against $1/L_{\text{min}}$ for different bond concentrations p , with L_{min} denoting the smallest lattice size used in the fits. We clearly see that in the regime of low dilution (p close to 1), the system is influenced by the pure fixed point. On the other hand, when the bond concentration is small, the vicinity of the percolation fixed point induces a decrease of $1/\nu$ below its expected disordered value. This is plausible since the percolation fixed point is characterized by $1/\nu \approx 1.12$ [24].

3.2 3D Bond-Diluted 4-State Potts Model

Let us now turn to the 4-state Potts model which exhibits in the pure case a rather strong first-order phase transition. In order to map out the phase diagram of the diluted model we considered all concentrations p in the interval $[0.28, 1]$ in steps of 0.04 and determined again the locations of the maxima of the susceptibility for a given lattice size L . The resulting phase diagram is depicted in Fig. 6, where we show for comparison again the simple mean-field prediction (3) and the effective-medium approximation (4), using $K_c(1) = 0.62863(2)$ [19]. On the scale of Fig. 6, estimates from high-temperature series expansions up to order 18 are hardly distinguishable, for a comparison see Ref. [23].

In a second step, the order of the phase transitions was investigated. Here, in order to satisfy our criterion $N_{\text{MCS}} > 250 \tau_e$, the number of MC sweeps had to be increased up to 15 000 – 30 000, which is rather large compared to the values used in the Ising case. A first indication is given by the FSS behaviour of the autocorrelation time τ_e at the transition point. A glance on the log-log plot of Fig. 7 shows a crossover around $p = 0.80$ from a power-law behaviour for strong disorder (small p) to a clear exponential behaviour for weak disorder ($p \approx 1$), as is typical for a first-order phase transition. In fact, in the latter case one expects $\tau_e \propto \exp(2\sigma_{od}L^2)$, where the (reduced) interface tension σ_{od} parameterizes the free-energy barrier separating the coexisting ordered and disordered phases.

In the first-order regime we performed multicanonical simulations and estimated the interface tension from

$$\sigma_{od} = \frac{1}{2L^2} \log \frac{P_{\max}}{P_{\min}}, \quad (7)$$

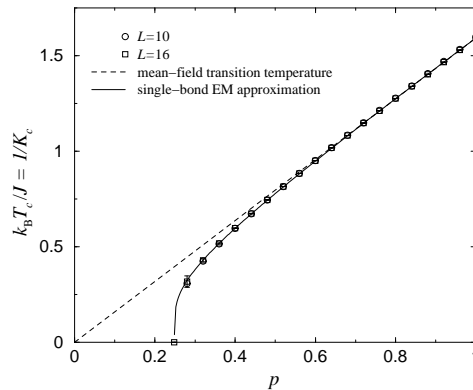


Fig. 6. Phase diagram of the 3D bond-diluted 4-state Potts model as obtained from MC simulations as well as the mean-field (dashed line) and single-bond effective-medium (solid line) approximations (3) and (4), respectively.

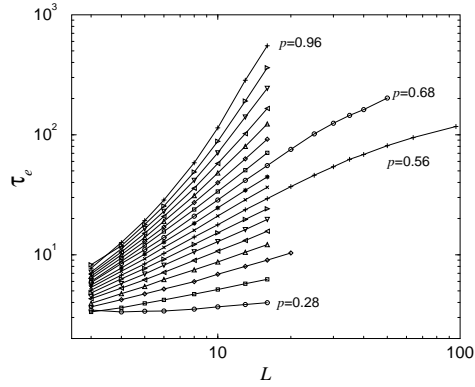


Fig. 7. Autocorrelation time τ_e of the energy at $K_c(p)$ versus lattice size L (p in steps of 0.04) for the 3D bond-diluted 4-state Potts model.

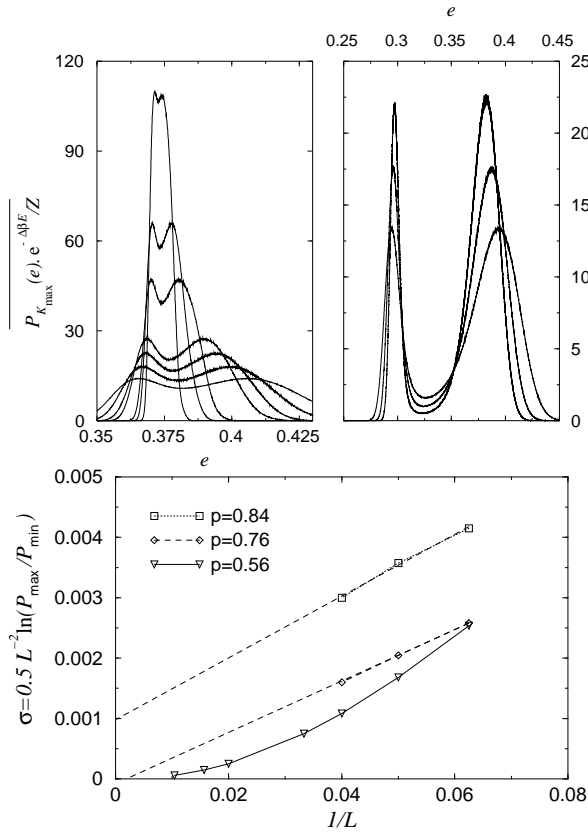


Fig. 8. Probability density of the energy of the 3D bond-diluted 4-state Potts model reweighted to equal peak height for $p = 0.56$ (top left) and $p = 0.84$ (top right). Interface tension versus inverse lattice size (bottom).

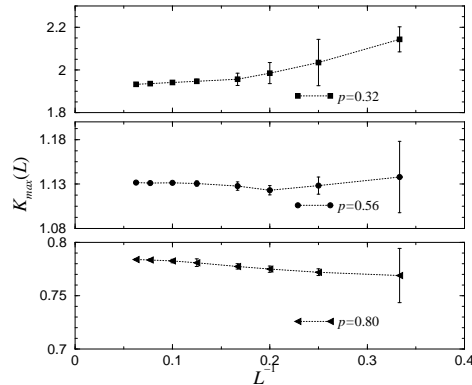


Fig. 9. FSS behaviour of the effective transition points for three different dilutions of the 3D 4-state Potts model as derived from the susceptibility maxima.

where P_{\max} is the maximum of the probability density reweighted to the temperature where the two peaks are of equal height, and P_{\min} is the minimum in between, see Fig. 8. The linear extrapolations of σ_{od} in $1/L$ in the lower part of Fig. 8 imply non-vanishing interface tensions only for $p = 0.84$ and above. For $p \leq 0.76$, σ_{od} seems to vanish in the infinite-volume limit, being indicative of the expected softening to a second-order phase transition. The tricritical point would thus be located around $p = 0.76 - 0.84$, in good agreement with the estimate of $p = 0.80$ derived from the analysis of autocorrelation times.

To confirm the softening for $p \leq 0.76$ we have performed a detailed FSS study at $p = 0.56$ with lattice sizes ranging up to $L = 96$ and the number of realisations varying between 2000 and 5000 [19]. The choice of $p = 0.56$ is motivated by our observation that in this range of dilutions the corrections to asymptotic FSS of the effective transition points are minimal, cf. Fig. 9.

The log-log plot for $\bar{\chi}_{\max}$ in Fig. 10 shows that for this quantity the corrections to asymptotic FSS seem to become quite small above $L = 30$, and fits of the form $a_{\chi}L^{\gamma/\nu}$ starting at $L_{\min} > 30$ yield $\gamma/\nu = 1.50(2)$. Using the data for $L < 30$ only, on the other hand, we obtained perfect fits assuming percolation exponents, $\gamma/\nu \approx 2.05$ [24], cf. Fig. 10. Similarly, the FSS of the quantity $(d \ln \bar{m}/dK)_{K_{\max}} \propto L^{1/\nu}$ gives for $L_{\min} > 30$ an estimate of the exponent $1/\nu = 1.33(3)$, consistent with the stability condition of the random fixed point ($1/\nu \leq D/2 = 1.5$) [29]. The same procedure was applied to the magnetization $\bar{m} \propto L^{-\beta/\nu}$, but here the associated critical exponent turned out to be not yet stable. We therefore also considered the FSS behaviour of higher (thermal) moments of the magnetization, $\overline{\langle \mu^n \rangle}$, which should scale with an exponent $n\beta/\nu$. The results for the first moments exhibit, however, again much stronger corrections to scaling than we observed for $\bar{\chi}$ or $d \ln \bar{m}/dK$, leading to quite a conservative final estimate of $\beta/\nu = 0.65(5)$.

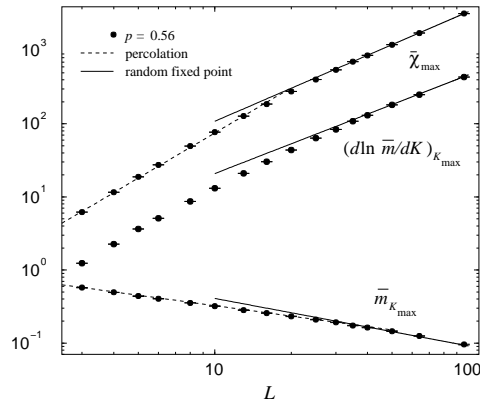


Fig. 10. FSS behaviour of the susceptibility, of $d \ln \bar{m}/dK$, and of the magnetization at K_{\max} for the 3D bond-diluted 4-state Potts model at $p = 0.56$ (the quantities have been shifted in the vertical direction for the sake of clarity). The scaling behaviour for small lattice sizes below a crossover length scale is presumably governed by the percolation fixed point.

We nevertheless note that our results do not fit satisfactorily the scaling law $2\beta/\nu = d - \gamma/\nu$. The reason could be the strong corrections to scaling at the random fixed point which are hard to cope with for medium-sized systems [19].

4 Conclusions

By performing large-scale Monte Carlo simulations we have investigated the influence of bond dilution on the critical properties of the 3D Ising and 4-state Potts models. In the 3D Ising case the universality class of the disordered model is modified by disorder but its precise characterization turned out to be difficult because of the competition between the different fixed points which induce crossover effects, even for relatively large lattice sizes.

Applying similar techniques to the 3D 4-state Potts model we obtained clear evidence for softening to a continuous transition at strong disorder, with estimates for the critical exponents of $\nu = 0.752(14)$, $\gamma = 1.13(4)$, and $\beta = 0.49(5)$ at $p = 0.56$. The analysis of both the autocorrelation time and the interface tension leads to the conclusion of a tricritical point around $p = 0.80$.

5 Acknowledgements

We would like to thank Meik Hellmund and Loic Turban for helpful discussions. The mutual visits within this collaboration were financially supported

by the joint PROCOPE exchange programme of the DAAD and EGIDE. C.C. thanks the EU network “EUROGRID: *Discrete Random Geometries: From solid state physics to quantum gravity*” for a post-doctoral position in Leipzig, and W.J. thanks the German-Israel-Foundation (GIF) for support. The numerical work would have been impossible without the computer-time grants 2000007 of the Centre de Ressources Informatiques de Haute-Normandie (CRIHAN), hlz061 of NIC, Jülich, and h0611 of LRZ, München. We are grateful to all institutions for their generous support.

References

1. Cardy, J. (1996): *Scaling and Renormalization in Statistical Physics*. Cambridge University Press Cambridge; chap. 8
2. Schwenger, L., Budde, K., Voges, C., Pfnür, H. (1994): *Phys. Rev. Lett.*, **73**, 296
3. Janke, W., Johnston, D.A. (2000): *Nucl. Phys. B*, **578**, 681; *J. Phys. A*, **33**, 2653
4. Harris, A.B. (1974): *J. Phys. C*, **7**, 1671
5. Selke, W., Shchur, L.N., Talapov, A.L. (1994): In: Stauffer, D. (ed) *Annual Reviews of Computational Physics I*. World Scientific Singapore; pp. 17–54
6. For a recent overview, see Folk, R., Holovatch, Y., Yavors’kii, T. (2001): e-print cond-mat/0106468
7. Imry, Y., Wortis, M. (1979): *Phys. Rev. B*, **19**, 3580
8. Aizenman, M., Wehr, J. (1989): *Phys. Rev. Lett.*, **62**, 2503
9. Chen, S., Ferrenberg, A.M., Landau, D.P. (1995): *Phys. Rev. E*, **52**, 1377
10. Picco, M. (1997): *Phys. Rev. Lett.*, **79**, 2998
11. Jacobsen, J.L., Cardy, J.L. (1998): *Nucl. Phys. B*, **515**, 701
12. Chatelain, C., Berche, B. (1998): *Phys. Rev. Lett.*, **80**, 1670
13. Olson, T., Young, A.P. (1999): *Phys. Rev. B*, **60**, 3428
14. Cardy, J., Jacobsen, J.L. (1997): *Phys. Rev. Lett.*, **79**, 4063
15. For a review, see Cardy, J. (1999): *Physica A*, **263**, 215
16. Ballesteros, H.G., Fernández, L.A., Martín-Mayor, V., Muñoz Sudupe, A., Parisi, G., Ruiz-Lorenzo, J.J. (2000): *Phys. Rev. B*, **61**, 3215
17. Janke, W., Villanova, R. (1997): *Nucl. Phys. B*, **489**, 679
18. Berche, P.-E., Chatelain, C., Berche, B., Janke, W. (2002): *Comp. Phys. Comm.*, **147**, 427
19. Chatelain, C., Berche, B., Janke, W., Berche, P.-E. (2001): *Phys. Rev. E*, **64**, 036120
20. Chatelain, C., Berche, P.-E., Berche, B., Janke, W. (2002): *Nucl. Phys. B (Proc. Suppl.)*, **106&107**, 899
21. Chatelain, C., Berche, P.-E., Berche, B., Janke, W. (2002): *Comp. Phys. Comm.*, **147**, 431
22. Hellmund, M., Janke, W. (2002): *Comp. Phys. Comm.*, **147**, 435
23. Hellmund, M., Janke, W. (2002): *Nucl. Phys. B (Proc. Suppl.)*, **106&107**, 923
24. Lorenz, C.D., Ziff, R.M. (1998): *Phys. Rev. E*, **57**, 230
25. Swendsen, R.H., Wang, J.S. (1987): *Phys. Rev. Lett.*, **58**, 86
26. Berg, B.A. (2000): *Fields Inst. Commun.*, **26**, 1

27. Janke, W. (1998): *Physica A*, **254**, 164
28. Derrida, B. (1984): *Phys. Rep.*, **103**, 29; Aharony, A., Harris, A.B. (1996): *Phys. Rev. Lett.*, **77**, 3700; Wiseman, S., Domany, E. (1998): *Phys. Rev. Lett.*, **81**, 22
29. Chayes, J.T., Chayes, L., Fisher, D.S., Spencer, T. (1986): *Phys. Rev. Lett.*, **57**, 2999; (1989): *Comm. Math. Phys.*, **120**, 501
30. Talapov, A.L., Blöte, H.W.J. (1996): *J. Phys. A*, **29**, 5727
31. Turban, L. (1980): *Phys. Lett. A*, **75**, 307; *J. Phys. C*, **13**, L13
32. Guida, R., Zinn-Justin, J. (1998): *J. Phys. A*, **31**, 8103
33. Ballesteros, H.G., Fernández, L.A., Martín-Mayor, V., Muñoz Sudupe, A., Parisi, G., Ruiz-Lorenzo, J.J. (1998): *Phys. Rev. B*, **58**, 2740
34. Varnashev, K.B. (2000): *Phys. Rev. B*, **61**, 14660
35. Pelissetto, A., Vicari, E. (2000): *Phys. Rev. B*, **62**, 6393